

1

2

Thermoconforming rays of the star-nosed mole

3

4

5

6 Glenn J. Tattersall^{1*} and Kevin L. Campbell²

7

8 ¹Department of Biological Sciences, Brock University, 1812 Sir Isaac Brock Way, St.

9 Catharines, Ontario, Canada L2S 3A1

10

11 ²Department of Biological Sciences, University of Manitoba, Winnipeg, Manitoba, Canada, R3T

12 2N2

13

14 *Author to whom correspondence should be addressed

15

16 Submitted to Journal of Experimental Biology as a Short Communication

17 **Summary Statement (for JEB Submission). 15-30 words**

18 The highly mechanosensitive nasal rays of the star-nosed mole conform closely with ambient

19 temperature thereby minimizing heat loss without apparent changes in sensory performance.

20 **Abstract**

21 The star-nosed mole (*Condylura cristata*) is well known for its unique star-like rostrum
22 ('star') which is formed by 22 nasal appendages highly specialised for tactile sensation. As a
23 northerly distributed insectivorous mammal occupying both aquatic and terrestrial habitats, this
24 sensory appendage is regularly exposed to cold water and thermally conductive soil, leading us
25 to ask whether the surface temperature, a proxy for blood flow to the star, conforms to the local
26 ambient temperature to conserve body heat. Alternatively, given the high functioning and
27 sensory nature of the star, we posited it was possible that the rays may be kept continually warm
28 when foraging, with augmented peripheral blood flow serving the metabolic needs of this tactile
29 sensory organ. To test these ideas, we remotely monitored the surface temperatures of the star
30 and other uninsulated appendages in response to changes in local water or ground temperature in
31 captive, wild-caught star-nosed moles. While the tail responded to increasing heat load through
32 vasodilation, the surface temperature of the star consistently thermoconformed, varying passively
33 in surface temperature, suggesting little evidence for thermoregulatory vasomotion. This
34 thermoconforming response may have evolved as a compensatory response related to the high
35 costs of heat dissipation to water or soil in this actively foraging insectivore.

36

37 **Keywords:** sensory organ, thermoregulation, insectivore, thermal window, thermography.

38 **Introduction**

39 The star-nosed mole (*Condylura cristata*) is a highly specialized insectivore that is uniquely
40 adapted to foraging in both terrestrial and aquatic habitats (Catania, 1999; Catania, 2000). Found
41 throughout eastern North America, and extending northward to the southern limit of permafrost,
42 this nearly blind predator primarily relies on its incredibly touch sensitive nasal appendages to
43 rapidly identify and consume hundreds of tiny prey items per day to fuel its high rate of
44 metabolism (Campbell et al., 1999; Catania and Remple, 2005). Owing to its distinctive
45 morphology, the eponymous nose ('star') of the star-nosed mole has been extensively studied for
46 its sensory functions (Catania, 2000; Gould et al., 1993; Sachdev and Catania, 2002; Sawyer et
47 al., 2014). The rostrum houses 22 separate rays, 11 per side, that sample the tactile environment
48 10-15 times per second while foraging (Gerhold et al., 2013). The star is highly vascularized
49 with two large non-muscularised blood sinuses occupying approximately 40% of the volume of
50 each ray. Capillaries are also evident throughout the dermis underlying the thousands of sensory
51 papillae (Eimer's organs) within each ray (van Vleck, 1965).

52 The star acts as the primary mechanosensory organ, with >100,000 myelinated nerve fibres
53 innervating the roughly 30 thousand Eimer's organs covering the surface of the nose (Catania,
54 1995; Catania, 1999). While all rays contribute to the remarkable tactile acuity of the star, the
55 inner most 11th ray serves as a mechanosensory fovea (Catania, 2011; Sachdev and Catania,
56 2002), and when foraging, moles will redirect their attention to allow this appendage to
57 investigate stimuli immediately prior to consumption. The speed of this behaviour is astonishing,
58 as star-nosed moles can locate, identify, and ingest prey items in as little as 102 ms, crowning
59 them as one of fastest eaters of the animal kingdom (Catania and Remple, 2005). In principle, the
60 sensory structures of endotherms are metabolically active and highly temperature sensitive

61 tissues that are expected to function more effectively when maintained at a warm and stable
62 temperature (Glaser and Kroger, 2017). The elephant's (*Loxodonta africana*) trunk, for example,
63 is the warmest part of the skin (Weissenboeck et al., 2010). During development, sensory nerves
64 provide a map for arterial growth through secretion of VEGF (Mukouyama et al., 2002), and thus
65 there may be a natural tendency for sensory activity to be associated with changes in blood flow,
66 leading to potential trade-offs between sensory response and energy supply (in the form of body
67 heat). Indeed, a precedence for thermal-sensory associations exists (Glaser and Kroger, 2017).
68 For example, the sensory vibrissae of seals have been shown to maintain high temperatures
69 owing to the high vascularity serving the underlying metabolically active sensory tissue and do
70 not demonstrate vasoconstriction in the cold (Dehnhardt et al., 1998). This continuously elevated
71 temperature helps maintain tactile sensitivity across a range of water temperatures that might
72 otherwise hamper neuron function. Similarly, the eye heater organ found in billfish (Carey,
73 1982) has been argued to have evolved as a means of enhancing central nervous system
74 functionality and enhanced sensory acuity in cold environments (Fritsches et al., 2005). The
75 enhanced visual acuity gained from maintaining the eye at an elevated temperature provides a
76 distinct reaction time advantage over their highly active, but ectothermic prey. On the other
77 hand, consider an ectothermic predator that senses heat; the pit organ of the pit viper is a highly
78 evolved infrared sensing tissue, consisting of a thin membranous tissue dense in mitochondria,
79 myelinated and unmyelinated nerves, and a high vascularity (Goris et al., 2007; Hisajima et al.,
80 2002). The latter has been argued to aid in providing rapid blood flow to help reduce after
81 images formed during heat sensing (Goris et al., 2007). Intriguingly, the infrared sensing
82 function of this tissue appears to operate better at cooler temperatures (Cadena et al., 2013),
83 although this may be related to the nature of the signal transfer rather than the sensory tissue

84 itself. Combined, there is reasonable precedence to expect that the nasal epidermal tissue of *C.*
85 *cristata* would show elevated temperatures based on high rates of blood flow supporting the
86 underlying metabolically active nervous tissues.

87 Endotherms typically have non-insulated or poorly insulated peripheral appendages that
88 tend to exhibit strong vasomotor control, reflective of their involvement in redistributing body
89 heat from the core to the periphery to aid in heat loss or to retaining heat in the core to aid in heat
90 conservation (Erdsack et al., 2012; Tattersall et al., 2012; Weissenboeck et al., 2010). Thermally,
91 these changes in blood flow can be assessed by examining how these uninsulated appendages’
92 surface temperatures change under different heat loads. This methodology has revealed classic
93 examples of adjustable thermal radiators that include elephant ears (Phillips and Heath, 1992),
94 the toucan bill (Tattersall et al., 2009), and rodent tails (Rand et al., 1965), to name a few. These
95 surfaces tend to contribute greatly to the body’s capacity to dissipate heat, but are also subject to
96 emotional influences, such as fear-induced vasoconstriction (Herborn et al., 2015; Vianna and
97 Carrive, 2005). In subterranean species, conductive heat loss to the soil is particularly high from
98 structures in direct contact with the substrate (see Plestilova et al., 2020). Given that the shallow
99 surface tunnels of star-nosed moles are typically excavated in water saturated soils, heat transfer
100 from the naked sensory appendages of the mole’s star is potentially extensive. This is especially
101 germane during the winter months when aquatic foraging by this species is more prevalent
102 (Campbell et al., 1999; Hamilton, 1931). Accordingly, due to the amphibious life history of the
103 star-nosed mole and the highly specialised sensory nature of its nasal rays, sustaining high rates
104 of warm arterial blood flow to the star may cause rapid heat loss and be energetically expensive
105 for the star-nosed mole to maintain.

106 We thus tested whether star-nosed moles keep their nasal sensory appendages warm
107 through vasodilation when exposed to the cold (thereby incurring high energetic costs) versus an
108 energy conservation hypothesis wherein despite its high vascularity, the uninsulated star will
109 show mainly passive warming and cooling responses (*i.e.*, thermoconformation). We did this by
110 exposing moles to different water temperatures and examining the patterns of surface
111 temperatures from their potential thermal windows (eye, tail, limbs, and nasal rays).

112

113 **Materials and Methods**

114 ***Animal Handling***

115 Three juvenile star-nosed moles of unknown sex were captured using Sherman and pitfall
116 traps in the Willard Lake region, Ontario (49° 49' 41.9088" N, 93° 58' 5.2896" W) in June 2022
117 under the authorization of an Ontario Ministry of Natural Resources Wildlife Scientific
118 Collector's permit (1101339). During their time in captivity (21 days), each mole was housed
119 within a two-chambered Rubbermaid system; one 76-L chamber, filled with moist soil to a depth
120 of ~15 cm housed a small wooden nesting enclosure that was connected via plastic (ABS) piping
121 to a second 76-L feeding chamber containing water to ~0.5 cm depth. Moles were allowed to
122 access to soil via an ABS tee wye attached to the nesting enclosure. Moles were fed
123 commercially sourced night crawlers (14-16 per day per animal) supplemented by wild-caught
124 earthworms and other invertebrates from the site of collection. The nesting chambers were
125 cleaned/replaced daily, while the feeding containers were thoroughly washed 2-3 times daily. All
126 procedures were approved by the Ontario Ministry of Northern Development, Mines, Natural
127 Resources and Forestry Wildlife Animal Care Committee (Protocol #22-493).

128 ***Thermal Manipulations***

129 Pilot observations conducted in air suggested that the nasal rays of the star-nosed mole
130 were heterothermic and closely corresponded to surface/air temperatures. We thus
131 experimentally exposed moles to warm (~30-32°C) or cold (2-4°C) water to elicit maximal
132 thermal responses. Briefly, individual moles were transferred to a clean 19-L Rubbermaid™
133 container held at room temperature (17-20°C) for 10 minutes (post-handling period), exposed to
134 warm or cold water at a depth of 1.5 cm for 10 minutes (water foraging period), and
135 subsequently transferred to a dry container for a further 10-minute recovery period in air at room
136 temperature. Each mole underwent this 30-minute procedure twice, once for each of the warm or
137 cold-water challenges. During the 10-min water exposure, moles were periodically provided with
138 earthworms (which were rapidly located and consumed regardless of water temperature) to
139 encourage natural underwater foraging behaviours.

140 ***Thermal Imaging***

141 Time lapse infrared thermal imaging videos were captured every second with FLIR
142 Research Studio software using a FLIR A8581 Mid-Wave Infrared Camera (resolution
143 1280x1024, 25 mm lens, thermal sensitivity <25 mK, accuracy ±1°C). The camera was mounted
144 ~0.5 m above the animal providing a full view throughout the measurement period. We assumed
145 emissivity of 0.95 and set object parameter settings in the software to the local air temperature
146 (~17-20°C). From the captured videos, we extracted still frames at various time points
147 throughout the post-handling, water foraging, and recovery periods. These still frames were
148 extracted as 32-bit TIF files and exported for analysis in FIJI/ImageJ (Schindelin et al., 2012).
149 Regions of interest were drawn over the front limbs, nose, nasal rays, eye, and tail using the free-
150 hand tool, and the average temperature for each region was extracted from each still frame.
151 Sample thermal images are depicted in Fig. 1.

152 **Data Analysis**

153 Acknowledging that the small sample size limits broad conjectures based on biologically
154 distinct replicates, we endeavoured to draw inferences of how various body part surface
155 temperatures differed from prevailing ground or water temperatures based on biophysical
156 principles outlined in Tattersall (2016). Surfaces that receive little blood flow or are insulated
157 from warm blood (*i.e.*, fur) are expected to be similar to local ground or water temperatures, and
158 due to principles of thermoconformity, should have slopes close to 1. This hypothesis was tested
159 using simple pairwise t tests (P values corrected using Bonferroni procedures for multiple
160 hypotheses). Surfaces that have high and non-varying blood flow are expected to deviate from
161 local temperature and to have a low slope ($\ll 1$) with respect to local temperature (tested by
162 model comparison to a model where the slope is set to 1 using the offset function in R).
163 Vasoactive body surfaces (*i.e.*, adjustable thermal windows), would differ from local temperature
164 when warm and exhibit a non-linear relationship with respect to local temperature, especially if
165 vasoconstricted in the cold and vasodilated under warm conditions. While the slope between
166 surface and local temperature may be less than 1, the obvious departure from linearity (tested by
167 comparing whether the more complex model significantly reduces the residual sums of squares
168 via a likelihood ratio test) reflects the vasoactive nature of the body surface. Statistical analyses
169 were conducted in R (version 4.2.0).

170

171 **Results**

172 Body surface temperatures of star-nosed moles were dependent on the ground and water
173 temperature but in varying manners (Fig. 1). The nasal rays and front limbs were primarily
174 thermoconforming body surfaces (Fig. 2 and Fig. 3) while the surface temperatures of the tail

175 and eyes tended to be elevated. Eye surface temperatures differed significantly from local
176 temperature ($t_{47}=9.4$; $P=9.03\times 10^{-12}$) and exhibited a slope significantly lower than 1 ($\chi^2_{df=1} =$
177 148 ; $P<2\times 10^{-16}$). The star and front limb temperatures were not significantly different than local
178 ambient temperatures ($t_{47}=-1.76$; $P=0.39$ and $t_{47}=-8.55\times 10^{-5}$; $P=1$, respectively), showing a
179 mostly linear, thermoconforming relationship. The tail was the most variable surface, being
180 significantly warmer than local temperature ($t_{47}=4.25$; $P=0.000580$) but also exhibiting a non-
181 linear relationship with local ground and water temperatures ($\chi^2_{df=1} = 8.9$; $P=0.0029$). Indeed, this
182 surface was warmest at mid-range ($\sim 20^\circ\text{C}$) temperatures and thermoconforming at higher and
183 lower temperatures (Fig. 3). While searching for food at room temperature, the nasal rays can be
184 seen to be close to the temperature of the ground surface (Movie 1 and 2). We only once
185 observed what might be evidence of vasodilation in the star that occurred during a prolonged,
186 relaxed grooming session (Movie 3).

187

188 **Discussion**

189 We demonstrated using surface temperature measurements that the nasal rays and
190 forelimbs of the star-nosed mole largely thermoconform to local water and ground temperatures,
191 providing support for an energy conservation role for the star, whereas the tail acts as an
192 adjustable thermal window, typical of many small mammals (Meyer et al., 2017; Rand et al.,
193 1965). For the most part then, the star acts passively in terms of vasomotor responsiveness, with
194 little evidence of vasodilation under heating scenarios; indeed, the nasal rays appear to be even a
195 little cooler than expected at the higher ambient temperatures, a response well characterised in
196 vampire bats (Kürten and Schmidt, 1982), canids (Balint et al., 2020), and numerous carnivores
197 (Glaser and Kroger, 2017).

198 Owing to linkages between skin temperature and tactile sensitivity, it has been argued
199 that cold rhinaria are incompatible with a mechanosensory role in mammals (Glaser and Kroger,
200 2017). Indeed, it is not unusual to expect warmer sensory structures to function more efficiently
201 given what has been described in facultatively endothermic animals (Carey, 1982; Fritsches et
202 al., 2005). However, canine olfactory-based tracking behaviours are enhanced at lower
203 temperatures and higher humidity's (Jinn et al., 2020), although this response has not been linked
204 to their typically cool nose temperature. Thus, the strikingly lower temperature of the star
205 relative to body temperature (37.7°C; Campbell et al., 1999) begs the question of whether this
206 trait aids or hinders the somatosensory function of the nasal rays while foraging. While not
207 systematically studied, observed reductions in star surface temperatures did not appear to be
208 associated with attendant reductions in prey detection ability as moles were able to rapidly locate
209 and consume added prey items in both warm and cold water. The bigger question then is how
210 does the star maintain high sensitivity/acuity in the cold if elevated blood flow and/or
211 temperatures are not involved? An important caveat here is that epithelial cells are the dominant
212 tissue of the rays, with much of the remaining volume composed of blood vessels and large
213 sinuses (van Vleck, 1965). Although thousands of nerve fibres are interspersed within each ray,
214 the cell bodies are located centrally within dorsal root ganglia. Accordingly, an argument for
215 high metabolic requirements demanding high blood flow (*e.g.*, Dehnhardt et al., 1998) seems
216 inadequate in the case of the star-nosed mole. However, hints regarding the thermoconforming
217 nature of the nasal star may be found in the specialised evolution of the sensory nerves
218 innervating the nose. The mole's nasal sensory nerves are of trigeminal ganglion origin and
219 enriched in the expression of ion channels involved in innocuous mechanosensation (CNGA2,
220 CNGA3, CNGA4, and FAM38a) compared to the expression pattern in dorsal root ganglia

221 innervating other parts of the body (Gerhold et al., 2013). By contrast, the trigeminal ganglia of
222 this species are deficient in the expression of ion channels typically associated with
223 thermosensation (TRPV1, TRPA1, TRPM8). Intriguingly, this same pattern was found in the
224 trigeminal neurons of the highly mechanosensitive bill of tactile-feeding waterfowl (ducks)
225 relative to visually foraging birds (Schneider et al., 2014). It was thus argued that the highly
226 specialised rostra of these species evolved to provide extremely high tactile sensitivity at the cost
227 of reduced thermosensation. However, since temperature sensing ion channels have been
228 implicated in the control of peripheral blood flow in mammals (Fromy et al., 2018), the reduction
229 of temperature sensing ion channels in the trigeminal ganglia, combined with the functional
230 thermoconforming evidence of the star provided herein, suggests an additional explanation.
231 Specifically, the low number of temperature sensing ion channels within the nasal epithelia that
232 have previously been linked to their intense anatomical specialisation for mechanosensation (see
233 Schneider et al., 2016) may also be related to the thermally non-responsive blood supply to the
234 star. In other words, the evolutionary diminution of temperature responding pathways may
235 prevent the reactive thermoregulatory vasomotion of this structure typically observed in
236 peripheral tissues of other endotherms. It should be stressed that, like star-nosed moles, tactile
237 feeding waterfowl that similarly possess low numbers of temperature-sensing neurons in their
238 bill do not exhibit reductions in feeding efficiency in the cold (Schneider et al., 2014). Taken
239 together, these observations suggest that evolutionary reductions in thermosensing ion channels
240 may be a specialization for somatosensory organs that must operate well below core body
241 temperatures. Curiously, an enhanced sensory response has been observed in the rattlesnake pit
242 organ when cold, as it responds more strongly to stimuli at cooler temperatures than at warm
243 temperatures (Bakken et al., 2018; Cadena et al., 2013).

244 A further explanation for why the star-nose mole shows low vasomotor responses in the
245 star and front limbs might also be related to the already substantial thermal window found in the
246 sparsely haired tail (Fig. 1). The star-nosed mole tail surface temperature response to handling
247 (see Fig. 1D) and changing environmental conditions correspond closely to that seen in rodent
248 tails (Johansen, 1962; Romanovsky et al., 2002), whereby handling and cold-exposure induces
249 vasoconstriction and warm exposure induces vasodilation (Rand et al., 1965; Vianna and
250 Carrive, 2005). However, the tail of star-nosed moles is unusual among talpids in that it is
251 relatively long and accumulates extensive fat stores during the fall and winter (Hamilton, 1931;
252 Petersen and Yates, 1980). Accordingly, this poorly insulated and high-surface-area appendage is
253 well suited to serve as the primary peripheral thermal window involved in adjustable heat
254 exchange. The eye temperature response, on the other hand provides a unique perspective into
255 the species functional morphology. The eyes of star-nosed moles are minute, have tiny optic
256 nerves, and are likely only used for light/dark discrimination (Catania, 1999; Petersen and Yates,
257 1980). However, eye surface temperatures were elevated and remained nearly constant across all
258 tested temperatures, demonstrating a continuous and high level of blood flow to an organ that has
259 been argued to serve only a minor contribution to overall sensory input.

260 A final unresolved question pertains to the mechanism underlying the poikilothermic
261 nature of the star. For example, while the reduction of thermosensitive neurons innervating the
262 star may in part underlie the lack of temperature-dependent vasomotion observed in this study, it
263 does not provide insights into how the star is able to achieve relative thermoconformity with
264 environmental temperatures. While it is possible this ability arises via the operation of
265 countercurrent heat exchangers in the rostral region, presence of these structures have not been
266 identified in previous anatomical studies of this species. Alternatively, this trait may result from

267 intermittent blood flow to the star arising from nasal ray movements. For instance, the nasal rays
268 are oriented perpendicular to the nose while foraging (Fig. 1A, B) though these structures are
269 shifted more or less parallel to the nose when the head is raised (Fig. 1K) and while the mole is
270 inactive. When not foraging, star-nosed moles were also routinely observed to exhibit repetitive
271 flexing and extension of the nasal rays and to ‘groom’ the star with the forepaws. While not
272 definitive, the latter behaviour coincided with a sudden increase in blood flow during one of our
273 experiments (Movie 3) and may be important for promoting blood flow to through the large
274 nasal sinuses in the nasal appendages. These competing mechanisms provide potentially fruitful
275 avenues of research on the thermal biology of this unusual insectivore.

276

277 ***Conclusions***

278 Unconventionally for a peripheral appendage, the nasal rays of the star-nosed mole show
279 little evidence of reactive vasodilation that other mammalian appendages often demonstrate. This
280 thermoconforming response may be related to the high energetic consequences of heat
281 dissipation in a typical peripheral tissue that would accompany the active foraging lifestyle of the
282 star-nosed mole. Since they spend much of their life foraging in environments of high thermal
283 conductance, any body heat reaching the star would be rapidly dissipated to the environment.
284 Extending these results to other “sensory specialists” could be of great interest. For example,
285 numerous ducks have highly sensitive mechanosensation in the bill yet still forage at variable
286 water temperatures (Schneider et al., 2014), the duck-billed platypus (*Ornithorhynchus anatinus*)
287 relies on an extensively innervated and presumably well vascularised bill for electroreception to
288 forage underwater (Scheich et al., 1986), while the echidna (*Tachyglossus aculeatus*) bill is a
289 specialised mechanosensory appendage (Proske et al., 1998). Whether these appendages also

290 demonstrate heat conservation through promiscuous vasoconstriction while foraging is unknown,
291 but the discovery of similar or divergent responses would shed light on the physiological
292 conservatism between how thermoregulatory vascular control has evolved to minimise
293 influences on the sensory systems.

294 **Acknowledgements**

295 We thank Josh Campbell for assistance with mole capture, and the British Broadcasting
296 Corporation Studios Natural History Unit for accommodating this study. This research was
297 supported by NSERC Discovery Grants to GJT (RGPIN-2020-05089) and KLC (RGPIN-2016-
298 06562) and an NSERC Research Tools and Instrumentation Grant to GJT (NSERC RTI-2021-
299 00278)

300

301 **Competing Interests**

302 No competing interests declared.

303

304

305 **Data availability**

306 <http://hdl.handle.net/10464/16980>

307

308 **Author Contributions**

309 Conceptualization: GJT and KLC; Investigation: GJT and KLC; Formal Analysis: GJT; Writing
310 – Original Draft Preparation: GJT and KLC; Writing – Review & Editing: GJT and KLC;
311 Visualization: GJT; Data Curation: GJT.; Funding Acquisition: GJT and KLC.

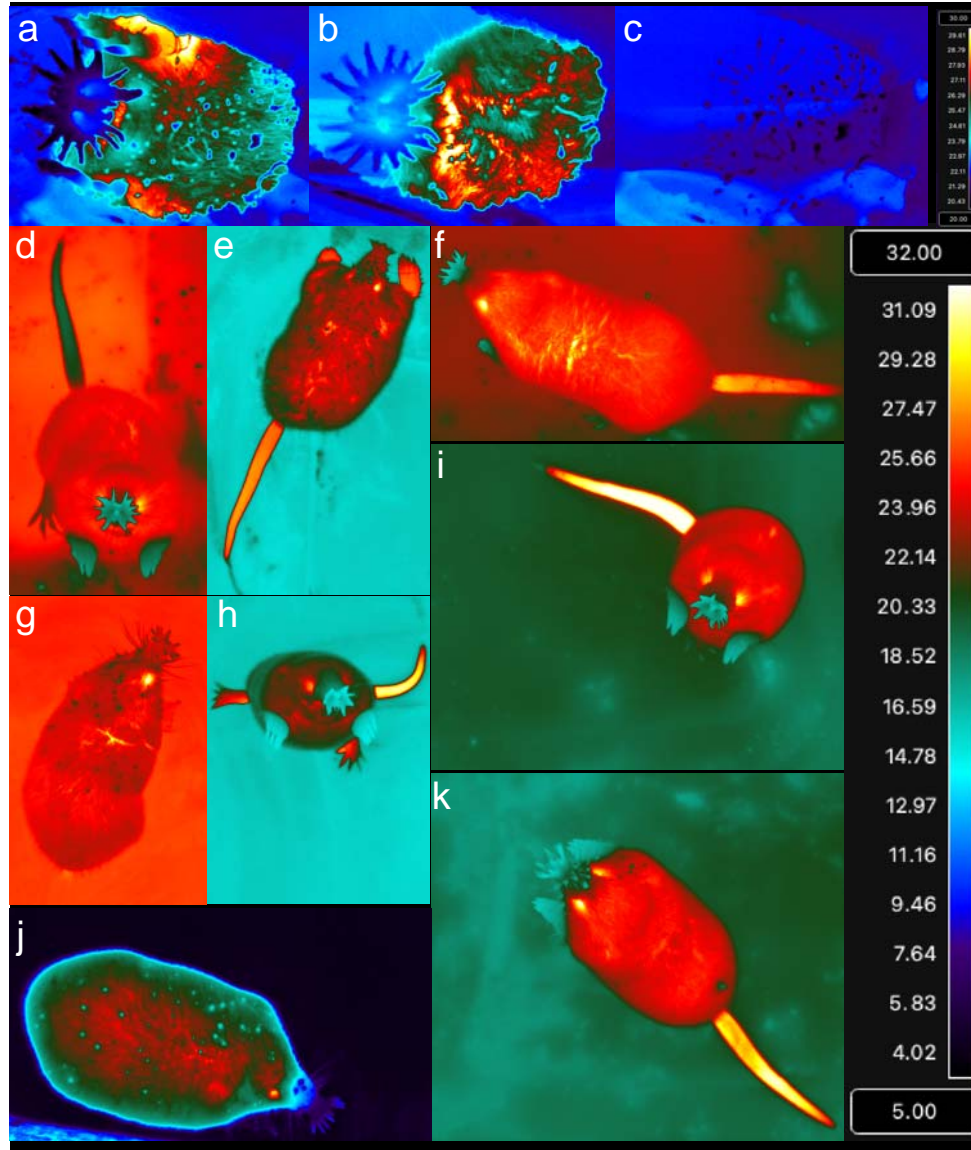
312 **References**

- 313
- 314 **Bakken, G. S., Schraft, H. A., Cattell, R. W., Tiu, D. B. and Clark, R. W.** (2018). Cooler
315 snakes respond more strongly to infrared stimuli, but we have no idea why. *Journal of*
316 *Experimental Biology* **221**, jeb182121.
- 317 **Balint, A., Andics, A., Gacsi, M., Gabor, A., Czeibert, K., Luce, C. M., Miklosi, A. and**
318 **Kroger, R. H. H.** (2020). Dogs can sense weak thermal radiation. *Scientific Reports* **10**,
319 3736.
- 320 **Cadena, V., Andrade, D. V., Bovo, R. P. and Tattersall, G. J.** (2013). Evaporative respiratory
321 cooling augments pit organ thermal detection in rattlesnakes. *Journal of Comparative*
322 *Physiology A* **199**, 1093-104.
- 323 **Campbell, K. L., McIntyre, I. W. and MacArthur, R. A.** (1999). Fasting metabolism and
324 thermoregulatory competence of the star-nosed mole, *Condylura cristata* (Talpidae:
325 Condylurinae). *Comparative Biochemistry and Physiology A Molecular Integrative*
326 *Physiology* **123**, 293-298.
- 327 **Carey, F. G.** (1982). A brain heater in the swordfish. *Science* **216**, 1327-1329.
- 328 **Catania, K. C.** (1995). Structure and innervation of the sensory organs on the snout of the star-
329 nosed mole. *Journal of Comparative Neurology* **351**, 536-548.
- 330 **Catania, K. C.** (1999). A nose that looks like a hand and acts like an eye: the unusual
331 mechanosensory system of the star-nosed mole. *Journal of Comparative Physiology A*
332 **185**, 367-372.
- 333 **Catania, K. C.** (2000). Epidermal sensory organs of moles, shrew moles, and desmans: a study
334 of the family talpidae with comments on the function and evolution of Eimer's organ.
335 *Brain Behavior and Evolution* **56**, 146-174.
- 336 **Catania, K. C.** (2011). The sense of touch in the star-nosed mole: from mechanoreceptors to the
337 brain. *Philosophical Transactions of the Royal Society of London B Biological Sciences*
338 **366**, 3016-3025.
- 339 **Catania, K. C. and Remple, F. E.** (2005). Asymptotic prey profitability drives star-nosed moles
340 to the foraging speed limit. *Nature* **433**, 519-522.
- 341 **Dehnhardt, G., Mauck, B. and Hyvarinen, H.** (1998). Ambient temperature does not affect the
342 tactile sensitivity of mystacial vibrissae in harbour seals. *Journal of Experimental Biology*
343 **201**, 3023-3029.
- 344 **Erdsack, N., Hanke, F. D., Dehnhardt, G. and Hanke, W.** (2012). Control and amount of heat
345 dissipation through thermal windows in harbor seals (*Phoca vitulina*). *Journal of Thermal*
346 *Biology* **37**, 537-544.
- 347 **Fritsches, K. A., Brill, R. W. and Warrant, E. J.** (2005). Warm eyes provide superior vision in
348 swordfishes. *Current Biology* **15**, 55-58.
- 349 **Fromy, B., Josset-Lamaugarny, A., Aimond, G., Pagnon-Minot, A., Marics, I., Tattersall,**
350 **G. J., Moqrish, A. and Sigauco-Roussel, D.** (2018). Disruption of TRPV3 impairs heat-
351 evoked vasodilation and thermoregulation: a critical role of CGRP. *J Invest Dermatol*
352 **138**, 688-696.
- 353 **Gerhold, K. A., Pellegrino, M., Tsunozaki, M., Morita, T., Leitch, D. B., Tsuruda, P. R.,**
354 **Brem, R. B., Catania, K. C. and Bautista, D. M.** (2013). The star-nosed mole reveals
355 clues to the molecular basis of mammalian touch. *PLoS One* **8**, e55001.
- 356 **Glaser, N. and Kroger, R. H. H.** (2017). Variation in rhinarium temperature indicates sensory
357 specializations in placental mammals. *Journal of Thermal Biology* **67**, 30-34.

- 358 **Goris, R. C., Atobe, Y., Nakano, M., Funakoshi, K. and Terada, K.** (2007). Blood flow in
359 snake infrared organs: response-induced changes in individual vessels. *Microcirculation*
360 **14**, 99-110.
- 361 **Gould, E., McShea, W. and Grand, T.** (1993). Function of the star in the star-nosed mole,
362 *Condylura cristata*. *Journal of Mammalogy* **74**, 108-116.
- 363 **Hamilton, W. J.** (1931). Habits of the star-nosed mole, *Condylura cristata*. *Journal of*
364 *Mammalogy* **12**, 345-355.
- 365 **Herborn, K. A., Graves, J. L., Jerem, P., Evans, N. P., Nager, R., McCafferty, D. J. and**
366 **McKeegan, D. E. F.** (2015). Skin temperature reveals the intensity of acute stress.
367 *Physiology & Behavior* **152**, 225-230.
- 368 **Hisajima, T., Kishida, R., Atobe, Y., Nakano, M., Goris, R. C. and Funakoshi, K.** (2002).
369 Distribution of myelinated and unmyelinated nerve fibers and their possible role in blood
370 flow control in crotaline snake infrared receptor organs. *Journal of Comparative*
371 *Neurology* **449**, 319-329.
- 372 **Jinn, J., Connor, E. G. and Jacobs, L. F.** (2020). How ambient environment influences
373 olfactory orientation in search and rescue dogs. *Chemical Senses* **45**, 625-634.
- 374 **Johansen, K.** (1962). Heat exchange through the muskrat tail. Evidence for vasodilator nerves to
375 the skin. *Acta Physiologica Scandinavica* **55**, 160-169.
- 376 **Kürten, L. and Schmidt, U.** (1982). Thermoperception in the common vampire bat (*Desmodus*
377 *rotundus*). *Journal of Comparative Physiology* **146**, 223-228.
- 378 **Meyer, C. W., Ootsuka, Y. and Romanovsky, A. A.** (2017). Body temperature measurements
379 for metabolic phenotyping in mice. *Frontiers in Physiology* **8**, 520.
- 380 **Mukouyama, Y. S., Shin, D., Britsch, S., Taniguchi, M. and Anderson, D. J.** (2002). Sensory
381 nerves determine the pattern of arterial differentiation and blood vessel branching in the
382 skin. *Cell* **109**, 693-705.
- 383 **Petersen, K. and Yates, T.** (1980). *Condylura cristata*. *Mammalian Species* **129**, 1-4.
- 384 **Phillips, P. K. and Heath, J. E.** (1992). Heat exchange by the pinna of the African elephant
385 (*Loxodonta africana*). *Comparative Biochemistry and Physiology* **101**, 693-699.
- 386 **Plestilova, L., Okrouhlik, J., Burda, H., Sehadova, H., Valesky, E. M. and Sumbera, R.**
387 (2020). Functional histology of the skin in the subterranean African giant mole-rat:
388 thermal windows are determined solely by pelage characteristics. *PeerJ* **8**, e8883.
- 389 **Proske, U., Gregory, J. E. and Iggo, A.** (1998). Sensory receptors in monotremes.
390 *Philosophical Transactions of the Royal Society of London B Biological Sciences* **353**,
391 1187-1198.
- 392 **Rand, R. P., Burton, A. C. and Ing, T.** (1965). The tail of the rat, in temperature regulation and
393 acclimatization. *Canadian Journal of Physiology and Pharmacology* **43**, 257-267.
- 394 **Romanovsky, A. A., Ivanov, A. I. and Shimansky, Y. P.** (2002). Selected contribution:
395 ambient temperature for experiments in rats: a new method for determining the zone of
396 thermal neutrality. *Journal of Applied Physiology* **92**, 2667-2679.
- 397 **Sachdev, R. N. and Catania, K. C.** (2002). Effects of stimulus duration on neuronal response
398 properties in the somatosensory cortex of the star-nosed mole. *Somatosensory & Motor*
399 *Research* **19**, 272-278.
- 400 **Sawyer, E. K., Leitch, D. B. and Catania, K. C.** (2014). Organization of the spinal trigeminal
401 nucleus in star-nosed moles. *Journal of Comparative Neurology* **522**, 3335-3350.
- 402 **Scheich, H., Langner, G., Tidemann, C., Coles, R. B. and Guppy, A.** (1986). Electroreception
403 and electrolocation in platypus. *Nature* **319**, 401-402.

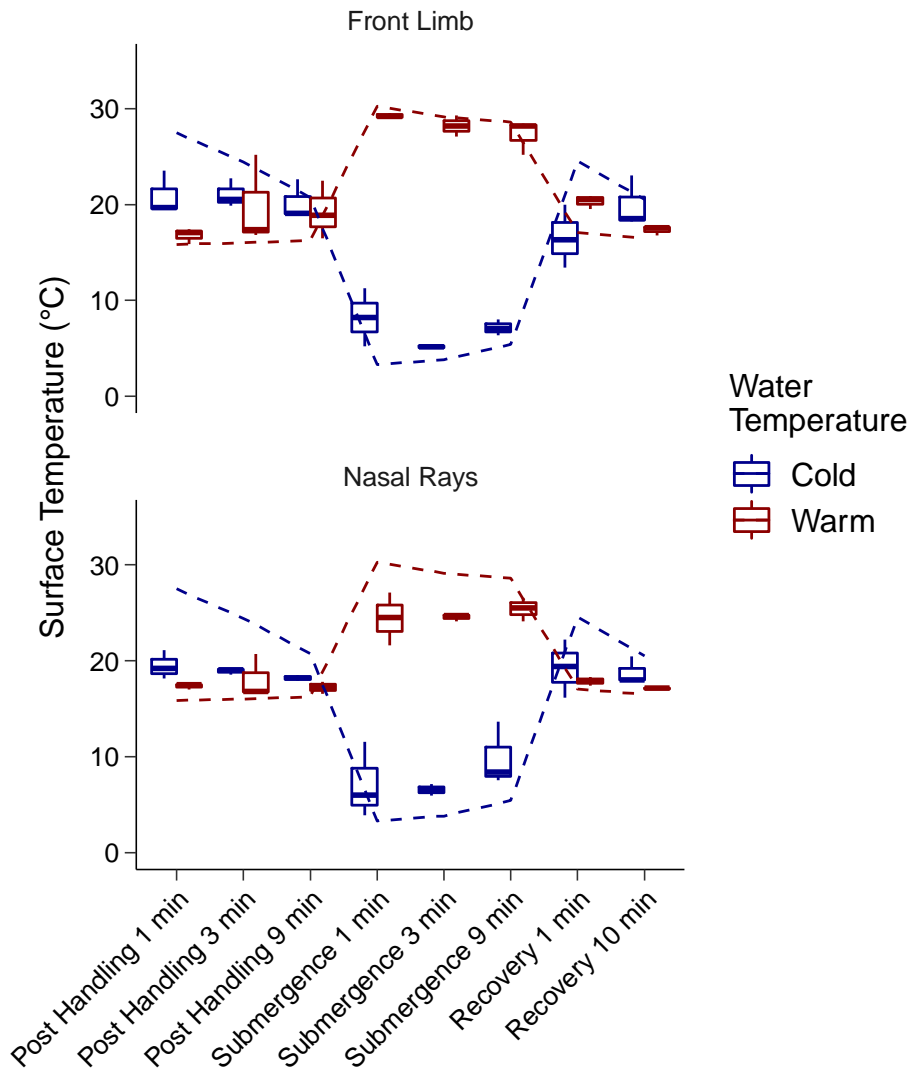
- 404 **Schindelin, J., Arganda-Carreras, I., Frise, E., Kaynig, V., Longair, M., Pietzsch, T.,**
405 **Preibisch, S., Rueden, C., Saalfeld, S., Schmid, B. et al.** (2012). Fiji: an open-source
406 platform for biological-image analysis. *Nature Methods* **9**, 676-682.
- 407 **Schneider, E. R., Gracheva, E. O. and Bagriantsev, S. N.** (2016). Evolutionary specialization
408 of tactile perception in vertebrates. *Physiology* **31**, 193-200.
- 409 **Schneider, E. R., Mastrotto, M., Laursen, W. J., Schulz, V. P., Goodman, J. B., Funk, O.**
410 **H., Gallagher, P. G., Gracheva, E. O. and Bagriantsev, S. N.** (2014). Neuronal
411 mechanism for acute mechanosensitivity in tactile-foraging waterfowl. *Proceedings of*
412 *the National Academy of Sciences USA* **111**, 14941-14946.
- 413 **Tattersall, G. J.** (2016). Infrared thermography: A non-invasive window into thermal
414 physiology. *Comparative Biochemistry and Physiology A Molecular Integrative*
415 *Physiology* **202**, 78-98.
- 416 **Tattersall, G. J., Andrade, D. V. and Abe, A. S.** (2009). Heat exchange from the toucan bill
417 reveals a controllable vascular thermal radiator. *Science* **325**, 468-470.
- 418 **Tattersall, G. J., Sinclair, B. J., Withers, P. C., Fields, P. A., Seebacher, F., Cooper, C. E.**
419 **and Maloney, S. K.** (2012). Coping with thermal challenges: physiological adaptations
420 to environmental temperatures. *Comprehensive Physiology* **2**, 2151-2202.
- 421 **van Vleck, D. B.** (1965). The anatomy of the nasal rays of *Condylura cristata*. *Journal of*
422 *Mammalogy* **46**, 248-253.
- 423 **Vianna, D. M. and Carrive, P.** (2005). Changes in cutaneous and body temperature during and
424 after conditioned fear to context in the rat. *European Journal of Neuroscience* **21**, 2505-
425 2512.
- 426 **Weissenboeck, N. M., Weiss, C. M., Schwammer, H. M. and Kratochvil, H.** (2010). Thermal
427 windows on the body surface of African elephants (*Loxodonta africana*) studied by
428 infrared thermography. *Journal of Thermal Biology* **35**, 182-188.
- 429

430 **Figures**
431

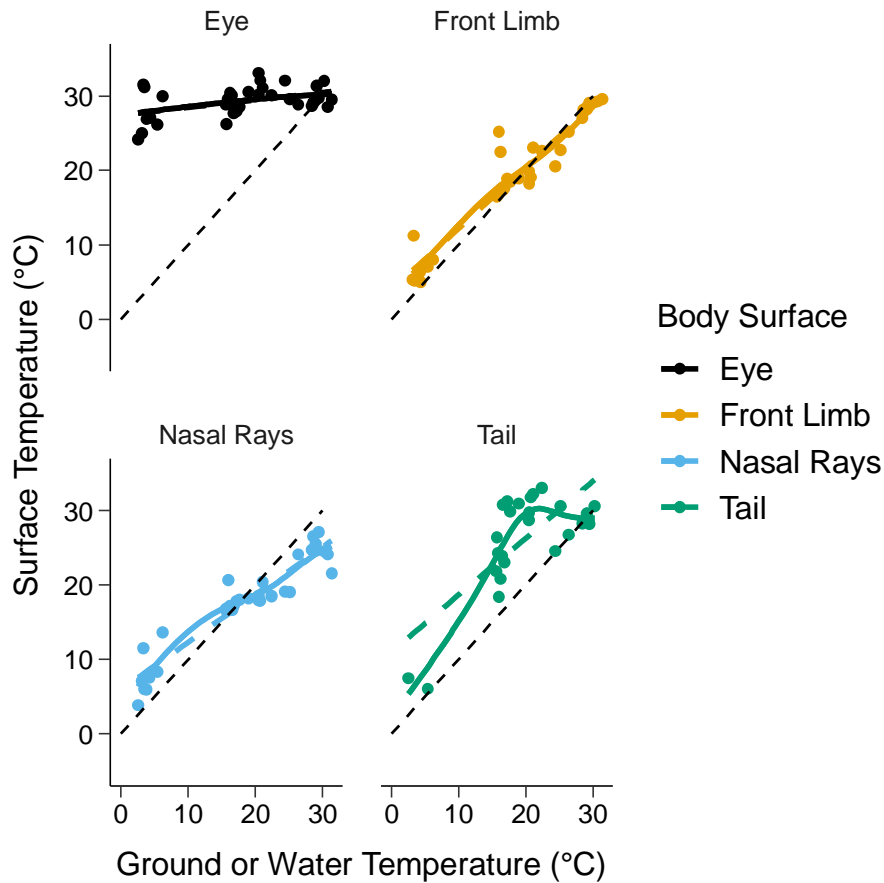


432
433
434
435
436
437
438
439
440
441
442
443
444
445

Figure 1. Representative thermal images of the star-nosed mole. Close-up image through a thin polyethylene sheet showing the warmer nostrils and distinctly cooler nasal rays when splayed out in surface contact (a,b) and the cool impressions (c) left behind at room temperature. Unless otherwise noted, the remaining images were captured during/after exposures to warm (~28-30°C) and cold (~2-4°C) environments. In d), immediately following handling after being placed into warm environment, e) immediate recovery at room temperature after exposed to warm water showing warm limbs, f) prior to being exposed to cold water while at room temperature, g) while foraging in warm water, h) recovery from exposure to warm water, i) and k) exposure to room temperature ground conditions, and j) during foraging in cold water. Note how the nasal ray and forelimb temperatures conform to ambient temperature while the eye and tail surface temperatures are generally much warmer. Temperature scale in upper right pertains to images a-c, while the larger temperature scale on the right pertains to images d-k.



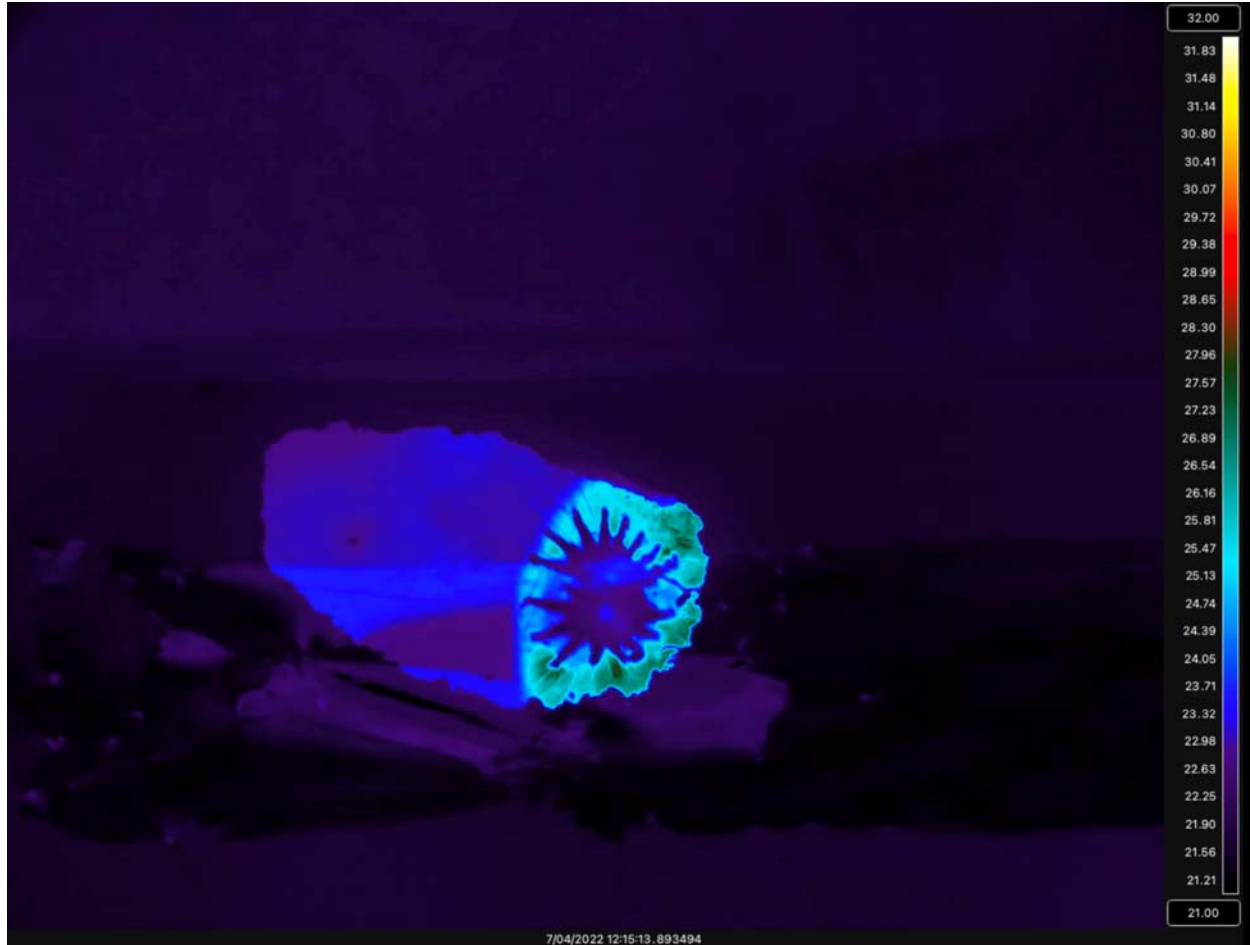
446
447 **Figure 2. Surface temperatures of the front limbs and nasal rays (foraging appendages)**
448 **prior, during, and following foraging in either cold (2-4°C) or warm (28-30°C) water.**
449 Symbols represent box and whisker plots (N=3), while the dotted lines represent the mean
450 ground or water temperature for the respective cold or warm water exposures.
451



452
453

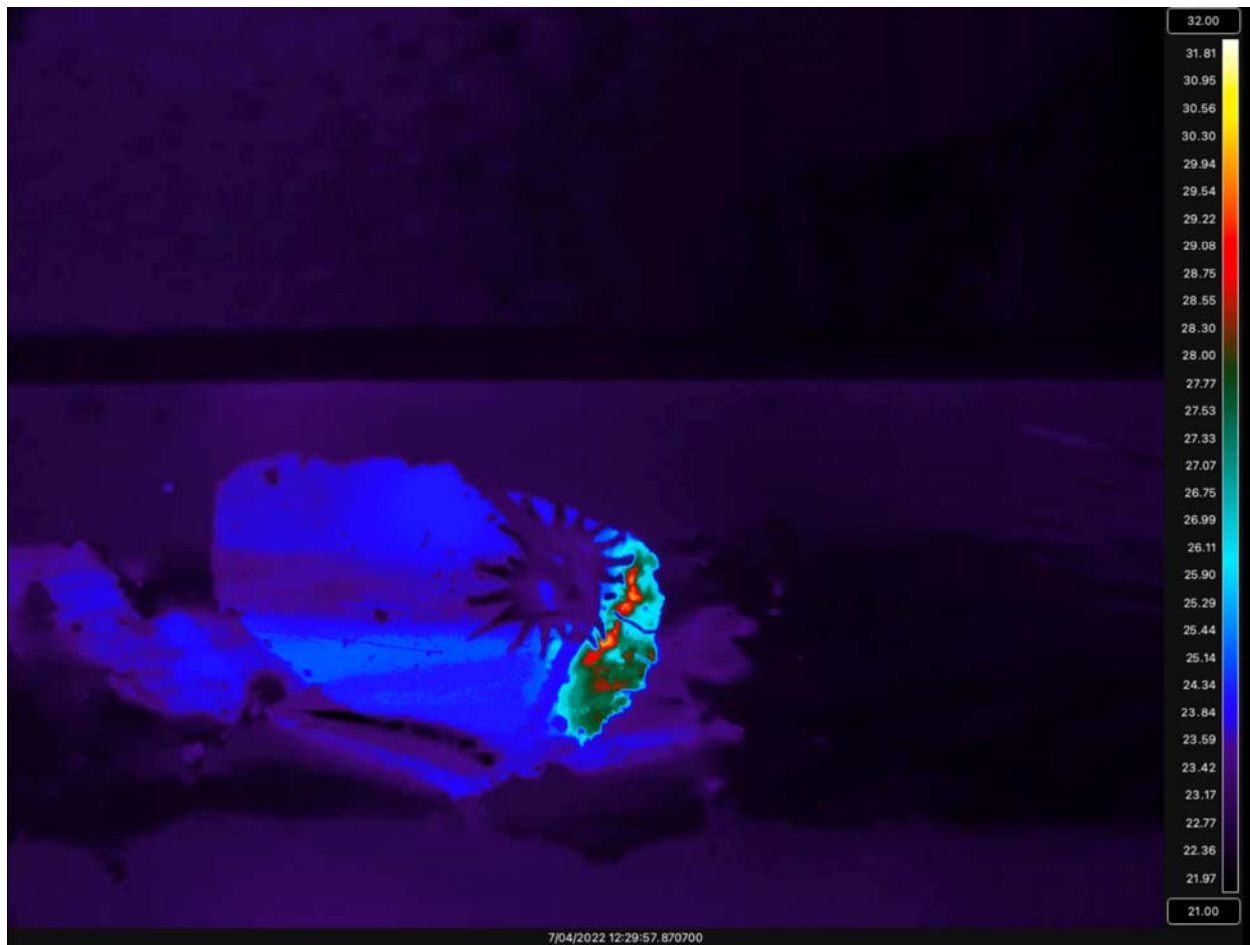
454 **Figure 3. Surface temperature relationships of exposed star-nosed mole surfaces relative to**
455 **ground or water temperatures across all measurement intervals.** The front limbs and nasal
456 rays are shown to mainly be thermoconforming surfaces. Eye surface temperature remained
457 warm across all temperatures while the tail showed a complex non-linear relationship reflective
458 of vasoconstriction in the cold and vasodilation at higher temperatures. Curves are included to
459 illustrate the non-linearity of most surface temperatures. Bold dashed lines depict the linear
460 regressions through the data, while the black dotted lines depict the line of equality.
461

462 **Supplementary Material**
463



464
465 **Movie 1.** Thermal video (48 frames/sec) of a star-nosed mole scanning an open surface, passing
466 over this surface in 0.48 seconds. The ‘window’ surface was a piece of plastic (Saran™ wrap)
467 stretched over a hole within an artificial tunnel environment.
468

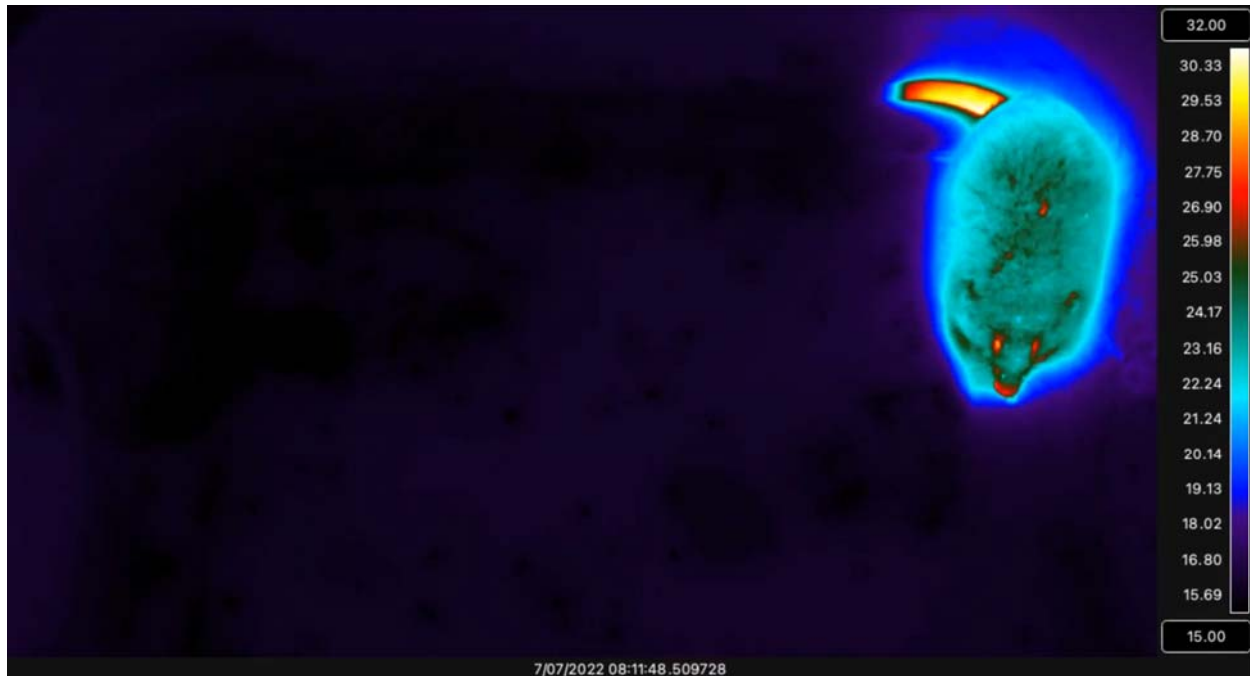
469



470

471

472 **Movie 2.** Thermal video (48 frames/sec) of a star-nosed mole scanning an open surface
473 containing a small earthworm, which was detected and consumed in under 3 seconds. The
474 ‘window’ surface was a piece of plastic (Saran™ wrap) stretched over a hole within an artificial
475 tunnel environment.



476
477

478 **Movie 3.** Time-lapse thermal video (frame rate 1 Hz, playback rate 10 Hz) of a star-nosed mole
479 grooming its nose. The star is not splayed open during grooming, and part-way through the video
480 (Timestamp 08:11:48.5, UTC +0), a sudden rise in nasal ray temperature is evident. Since the
481 front limbs are also warm during this video, it is not clear if heat is being transferred from the
482 limbs or if this arises from vasodilation of the nasal rays.